Distributionally Robust Scheduling of Integrated Gas-Electricity Systems with Demand Response

Chuan He, Member, IEEE, Xiaping Zhang, Member, IEEE, Tianqi Liu, Senior Member, IEEE, Lei Wu, Senior Member, IEEE

Abstract— This paper proposes a distributionally robust scheduling model for the integrated gas-electricity system (IGES) with electricity and gas load uncertainties, and further studies the impact of integrated gas-electricity demand response (DR) on energy market clearing as well as locational marginal electricity and gas prices (LMEPs and LMGPs). The proposed model maximizes the base-case system social welfare (i.e., revenue from price-sensitive DR loads minus energy production cost) minus the worst-case expected load shedding cost. Price-based gas-electricity DRs are formulated via price-sensitive demand bidding curves while considering DR participation levels and energy curtailment limits. By linearizing nonlinear Weymouth gas flow equations via Taylor series expansion and further approximating recourse decisions as affine functions of uncertainty parameters, the formulation is cast into a mixed-integer linear programming problem to enhance computational tractability. Case studies illustrate effectiveness of the proposed model for ensuring system security against uncertainties, avoiding potential transmission congestions, and increasing financial stability of DR providers.

Index Terms— Integrated gas-electricity systems, co-optimization, demand response, distributionally robust optimization.

NOMENCLATURE

Major symbols and notations used throughout the paper are defined below, while others are defined following their first appearances as needed.

Indices:

c, g, j	Index of gas compressors/gas loads/gas suppliers.
d, i, t	Index of electricity loads/units/hours.
e, m	Index of electricity grid buses/gas network nodes.
l, p	Index of power lines/gas pipelines.
k, n	Index of segments/breakpoints.

Variables:

f_{pt}^+, f_{pt}^-	Binary variables to indicate gas flow direction of
	pipeline p at time t .
G_{it}	Gas consumption of gas-fired unit <i>i</i> at time <i>t</i> .
G_{pt} , G_{ct}	Gas flow of pipeline p / compressor c at time t .
I_{it}	Commitment status of unit <i>i</i> at time <i>t</i> .
P_{ikt}	Power generation at segment k of unit i at time t .
P_{dkt} , G_{gkt}	Demand at segment k of electricity load d / gas load g
	at time t.
P_{it} , G_{jt}	Production of unit i/g as supplier j at time t .
P_{lt}, θ_{et}	Power flow of line l / phase angle of bus e at time t .
P_{dt}, G_{gt}	Scheduled electricity load d / gas load g at time t .
$P_{dt}^{\mathrm{dr}}, G_{gt}^{\mathrm{dr}}$	Adjustable electricity load d / gas load g at time t .

C. He and T. Liu are with the College of Electrical Engineering and Information Technology, Sichuan University, Chengdu, 610065, China (e-mail: he chuan@ scu.edu.cn, tqliu@scu.edu.cn). X. Zhang is with California Independent System Operator, Folsom, CA, 95630, USA (e-mail: xzhan126@hawk.iit.edu). L. Wu is with the ECE Department, Stevens Institute of Technology, Hoboken, NJ, 07030, USA (e-mail: lei.wu@stevens.edu).

 SU_{it} , SD_{it} Startup/shutdown fuel consumption of unit i at time t.

Slack variables indicating load shedding v_{dt}, v_{gt} electricity load d/ natural gas load g at time t. $X_{it}^{\text{on}}, X_{it}^{\text{off}}$ $X_{dt}^{\text{on}}, X_{dt}^{\text{off}}$ $X_{gt}^{\text{on}}, X_{gt}^{\text{off}}$ ON/OFF time counter of unit i at time t. ON/OFF time counter of electricity load d at time t. ON/OFF time counter of gas load g at time t. Y_{dt} , Y_{gt} Curtailment status of electricity load d/ gas load g, which is 1 if load is curtailed, being 0 otherwise. Pressure of gas node *m* at time *t*. π_{mt}

Constants:

Incremental fuel consumption at segment k of unit i. C_i^{fuel} , N_i Fuel price/ no-load fuel consumption of unit i. Bidding price at segment k of electricity load d/ gas C_{dkt} , C_{gkt} load *g* at time *t*.

 C_j Production cost of gas supplier j. C_d^{voll} , C_g^{voll} Load shedding penalty cost of electricity load d/Production cost of gas supplier *j*.

natural gas load g. K_p Gas flow constant of pipeline p.

MA large enough number.

 P_{dt}^{load} , G_{gt}^{load} Expected electricity load d/ gas load g at time t.

 su_i , sd_i Startup/shutdown cost of unit i. $T_i^{\text{on}}, T_i^{\text{off}}$ Minimum ON/OFF time of unit *i*.

 $T_d^{\text{on}}, T_d^{\text{off}}$ Minimum ON/OFF time of electricity load d.

 $T_g^{\text{on}}, T_g^{\text{off}}$ Minimum ON/OFF time of gas load g.

 UR_i,DR_i Ramp up/down rate of unit i. Reactance of transmission line *l*.

DR participation level of electricity load d/gas load g α_{dt} , α_{gt}

 Γ_c Compression factor of comp. (·)min/max Min/max value of a quantity. Compression factor of compressor c.

Sets and functions:

GUSet of gas-fired units. Set of components at electricity bus e/gas node m. N(e),N(m)Sending/receiving ends of power lines or pipelines. $s(\bullet), r(\bullet)$ $\Omega_E,\Omega_I,\Omega_L$ Sets of power buses, units, and power lines. $\Omega_M, \Omega_C, \Omega_P$ Sets of gas nodes, compressors, and pipelines. Ω_D, Ω_G Sets of electricity loads and gas loads. Ω_{J} , Ω_{K} , Ω_{T} Sets of gas suppliers, segments, and time periods.

I. Introduction

Natural gas-fired units have become the top choice for new generation expansion of power systems due to the lower cost, higher efficiency, and faster response capabilities [1]. The growing large fleet of gas-fired generators has intensified the interconnections of electricity grid and natural gas network [2]. That is, gas-fired units rely on just-in-time gas supply from the natural gas network, which has raised significant challenges on the operational security and efficiency of both systems. In turn,

modeling and optimizing them as an integrated gas-electricity system (IGES) could achieve a more secure and economic operations of both systems. In addition, DR programs in power systems have been successfully developed to flatten the load profile by transferring flexible demands away from peaks to lightly-loaded hours for enhancing energy reliability and efficiency [3]-[4]. On the contrary, natural gas DR has been underexplored. In fact, Whitehouse and other groups have recently started seeking for natural gas DR programs to help reduce costs for energy consumers [5]-[6]. Advantages of gas DR in the IGES include: (i) reducing electricity and gas price spikes and improving reliability of IGES; (ii) providing environmental benefits by making more clean natural gas fuel available to gas-fired units; and (iii) driving value by deferring or avoiding costly investments.

The day-ahead co-optimization scheduling of IGES has been discussed in [7]-[13] to ensure reliable and economic operations. A novel mixed-integer linear programing (MILP) model is proposed in [7] to study energy adequacy of IGES in short-term operations. Reference [8] applies new dynamic gas flow control techniques to examine day-ahead operations of generators and gas compressors in different coordination scenarios. A multi-area integrated electricity-natural gas model is presented in [9], which is solved in a decentralized manner to achieve decision autonomy of multiple participating areas. Moreover, as uncertainties within the IGES bring new challenges in the day-ahead scheduling, stochastic day-ahead scheduling considering volatile wind energy is proposed in [10]. Reference [11] presents two interval methods to study the impact of wind power uncertainty on the operation of electricity and natural gas systems. Robust optimization is also applied to the co-optimization scheduling of IGES considering power system uncertainties and natural gas system dynamics [12]. Reference [13] integrates transmission network N-1 contingencies in the robust scheduling model to ensure the operation security of IGES with wind power.

Demand-side participation could offer valuable options to set efficient energy prices, improve economic efficiency, and increase energy security. DR programs have been intensively studied in power systems. The impact of priced-based DR on market clearing and locational marginal prices (LMPs) is carried out in [3]. Reference [4] proposes a stochastic day-ahead scheduling model of power systems considering hourly DR. However, research regarding DR programs in IGES is rather limited. Interruptible-load based and coupon-based DR virtual power plants are considered in the coordinated operation of electricity grid and natural gas network in [14]. Electricity DRs with shifting capabilities are introduced in [15] to seek for economic day-ahead scheduling of the power system while considering gas transmission limits. Reference [16] models incentive electricity and gas DRs as linear functions of compensation prices to evaluate their effects on IGES operation.

From existing literature we notice that: (i) Distributionally robust optimization has been used in power system operations for handling uncertainties [17-20]. However, most works focus on optimizing first-stage unit commitment cost and second-stage worst-case expected dispatch cost. In addition, prior works on distributionally robust day-ahead scheduling of integrated gas-electricity systems are rather limited; (ii) Interruptible based, coupon-based, and incentive-based gas DRs

are considered in [14], [16], while priced-based gas DRs are not fully addressed; (iii) The impacts of integrated gas-electricity DRs on energy market clearing as well as LMEPs and LMGPs have not been investigated.

This paper proposes a distributionally robust co-optimization scheduling model for the coordinated optimal operation of electricity and natural gas systems, while considering uncertainties of electricity and gas loads. In addition, hourly price-based integrated gas-electricity DR is modeled for the first time to reduce peak load periods, flatten hourly load profiles, and provide economic operations [4], [15]. Specifically, the proposed model explores opportunities of utilizing natural gas DR to secure gas supply to gas-fired units and relieve power shortage of the electricity system, especially in critical circumstances such as peak electricity loads in summer.

The major contributions of this paper are twofold.

- 1) The paper proposes a two-stage distributionally robust co-optimization model for the day-ahead scheduling of IGES while considering uncertainties of electricity and natural gas loads. Instead of optimizing the worst-case expected system social welfare, the base-case system social welfare minus the worst-case expected load shedding cost is optimized to derive useful economic dispatch solutions in the day-ahead market and simultaneously guaranteeing system security.
- 2) Price-based integrated gas-electricity DR is considered as an economic option in the day-ahead scheduling of IGES for the first time, by shifting loads at peak hours to off-peaks. Similar to the concept of LMP in power systems, locational marginal electricity/gas prices (LMEPs and LMGPs) for IGES are proposed. Furthermore, benefits of price-based gas-electricity DRs on the operation of IGES and LMEPs/LMGPs are quantitatively analyzed via the proposed distributionally robust scheduling model.

The remainder of the paper is as follows. Sections II and III discuss the deterministic co-optimization scheduling model and its distributionally robust counterpart. Sections IV gives solution methodology. Numerical case studies are presented in Section V, and conclusions are given in Section VI.

II. DETERMINISTIC SCHEDULING MODEL

A. Formulation of the Deterministic Scheduling Model

In this paper, electricity system and natural gas system are considered as an integrated energy system with one system operator. A full co-ordination between electricity and natural gas system could increase the reliability and operation efficiency of both energy systems. On the other hand, a fully decentralized way to coordinate electricity and natural gas systems via alternating direction method of multipliers (ADMM) could be adopted to achieve decision independency and information privacy of the two energy systems [9], [12].

The deterministic scheduling model is to maximize the system social welfare of supplying hourly electricity and natural gas loads. The objective function (1) consists of revenue from DR loads minus load shedding penalty and production cost of IGES (revenue from inelastic loads is constant and thus neglected). The production cost of IGES includes gas production cost and production cost of non-gas thermal units. Note that production costs of gas-fired units are considered in terms of gas fuel cost and carried out by the gas production cost of gas suppliers. The

decision variables in the model include unit commitment statuses, gas flow directions, dispatches of the IGES, among others. Indeed, all variables presented in the nomenclature are decision variables of the deterministic scheduling model.

Power system constraints include minimum ON/OFF time limits (2)-(3), startup and shutdown costs (4)-(5), system load balance (6), generation limits (7)-(9), ramp up and down limits (10)-(11), DC power flow equations (12)-(13) in which power flow of a transmission line is calculated by bus angles and the line impedance, and bus angle limits (14). As a key component that couples electric power system and natural gas system, gas consumption of a gas-fired unit is calculated in (15) where HHV represents higher heating value that equals 1.026MBtu/kcf.

Constraints (16)-(23) describe power system DRs, adopting price-sensitive consumption curves to simulate price responsive loads. Here, price responsive loads could be curtailed or shifted to other operation hours in response to market prices. As energy consumption of a price responsive load would decrease monotonically with the increase in electricity price, in this paper, a stepwise DR bidding curve as shown in Fig. 1 is used to represent changes of price responsive load with respect to electricity price changes. The range of DR participation level α_{dt} is [0, 1]. That is, the inelastic load level is $(1-\alpha_{dt}) \cdot P_{dt}^{\text{load}}$. Minimum on/off constraints (16)-(17) of electricity load d define that certain load must be supplied/off for a number of consecutive hours after it is restored/curtailed [4], [15]. The relationship among scheduled load, adjustable load, and load segment variables is presented in (18)-(19). Constraint (20) defines limits of load segment variables. The range of adjustable load P_{dt}^{dr} is expressed in (21)-(22). Binary indicator Y_{dt} describes the status of DR load d at time t. Specifically, if Y_{dt} equals to 1, adjustable load P_{dt}^{dr} is positive, indicating that load d is curtailed/shifted at time t; When Y_{dt} is 0, negative adjustable load P_{dt}^{dr} means that load d is increased with demand from other hours shifted in at time t. The total curtailment of price responsive load d is limited by certain quantity (23). A positive setting of E_d^{max} indicates that a total amount of energy E_d^{max} at load d could be curtailed; If it is set as 0, it means that all reduced load at certain time periods will be fully shifted to other time periods.

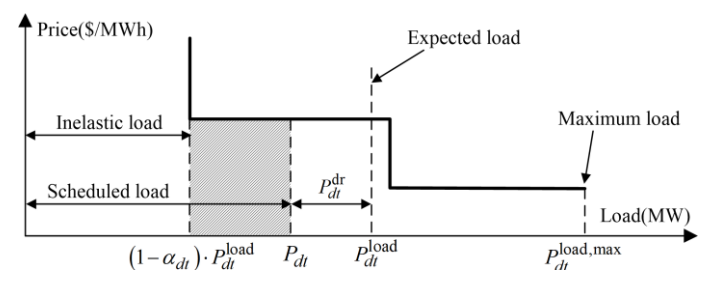


Fig. 1 A stepwise demand response curve.

As the largest complex networked systems, electricity and natural gas systems share certain similarities. Operation constraints of natural gas system are presented in (24)-(42). Gas network nodal balance equation is described in (24). Equations (25)-(26) defines limits of gas supplier productions and nodal pressures, respectively. The nonlinear relationship between nodal pressures and pipeline gas flows is described via Weymouth equations (27). Constraints (28)-(30) determine gas

flow directions of pipelines, where $f_{pl}^+=1/f_{pl}^-=1$ indicates that gas flows have positive/negative directions in pipeline p. Equation (31) calculates terminal gas pressures of compressor stations, where constraint (32) restricts gas flow directions in compressor stations. Similar to the modeling of electricity DRs in (16)-(23), price responsive natural gas DR load is analogously modeled via (33)-(40). Constraints (41)-(42) restrict values of electricity and gas load shedding variables.

$$\begin{aligned} & \max \sum_{l} \sum_{k} \sum_{\Delta_{l}} \sum_{k} C_{dkl} \cdot P_{dkl} + \sum_{g} \sum_{k} C_{gkl} \cdot G_{gkl} \cdot \sum_{l} C_{J} \cdot G_{J} \cdot \sum_{g} C_{gl}^{voll} \cdot v_{dl} - \sum_{l} c_{GU} C_{i}^{fucl} \cdot [\sum_{k} c_{Jk} \cdot P_{lkl} + N_{l} \cdot I_{ll} + SU_{ll} + SD_{ll}] \} \\ & \text{s.t.}(X_{i,l-1}^{v-1} - T_{i}^{on}) \cdot (I_{l,i-1} - I_{ll}) \geq 0, & i \in \Omega_{l}, t \in \Omega_{T} \quad (2) \\ & (X_{i,l-1}^{vol} - T_{i}^{ool}) \cdot (I_{l} \cdot I_{l,l-1}) \geq 0, & i \in \Omega_{l}, t \in \Omega_{T} \quad (3) \\ & SU_{ll} \geq sU_{l} \cdot (I_{l} \cdot I_{l,l-1}) \cdot SU_{ll} \geq 0, & i \in \Omega_{l}, t \in \Omega_{T} \quad (4) \\ & SD_{ll} \geq sU_{l} \cdot (I_{l} \cdot I_{l,l-1}) \cdot SU_{ll} \geq 0, & i \in \Omega_{l}, t \in \Omega_{T} \quad (4) \\ & SD_{ll} \geq sU_{l} \cdot (I_{l} \cdot I_{l,l-1}) \cdot SU_{ll} \geq 0, & i \in \Omega_{l}, t \in \Omega_{T} \quad (4) \\ & SD_{ll} \geq sU_{l} \cdot (I_{l} \cdot I_{l,l-1}) \cdot SU_{ll} \geq 0, & i \in \Omega_{l}, t \in \Omega_{T} \quad (4) \\ & SD_{ll} \geq sU_{l} \cdot (I_{l} \cdot I_{l,l-1} \cdot I_{ll}) \cdot SU_{ll} \geq 0, & i \in \Omega_{l}, t \in \Omega_{T} \quad (4) \\ & SD_{ll} \geq sU_{l} \cdot (I_{l} \cdot I_{l-1} \cdot I_{l}) \cdot SU_{ll} \geq 0, & i \in \Omega_{l}, t \in \Omega_{T} \quad (4) \\ & SD_{ll} \geq sU_{l} \cdot (I_{l} \cdot I_{l-1} \cdot I_{l}) \cdot SU_{ll} \geq 0, & i \in \Omega_{l}, t \in \Omega_{T} \quad (4) \\ & SD_{ll} \geq SU_{l} \cdot (I_{l} \cdot I_{l-1} \cdot I_{l}) \cdot SU_{ll} \geq 0, & i \in \Omega_{l}, t \in \Omega_{T} \quad (4) \\ & SD_{ll} \geq SU_{l} \cdot (I_{l} \cdot I_{l-1} \cdot I_{l}) \cdot SU_{l} \geq 0, & i \in \Omega_{l}, t \in \Omega_{T} \quad (4) \\ & SD_{ll} \geq SU_{l} \cdot (I_{l} \cdot I_{l-1} \cdot I_{l}) \cdot SU_{l} \cdot$$

$$\begin{aligned} & - \left(1 - Y_{gt} \right) \cdot M \leq G_{gt}^{\text{dr}} \leq \alpha_{gt} \cdot G_{gt}^{\text{load}} + \left(1 - Y_{gt} \right) \cdot M, \ g \in \Omega_G, t \in \Omega_T \ (38) \\ & - Y_{gt} \cdot M + G_{gt}^{\text{load}} - G_{gt}^{\text{load}, \max} \leq G_{gt}^{\text{dr}} \leq Y_{gt} \cdot M, \quad g \in \Omega_G, t \in \Omega_T \ (39) \\ & 0 \leq \sum_t G_{gt}^{\text{dr}} \leq E_g^{\text{max}}, \qquad \qquad g \in \Omega_G, t \in \Omega_T \ (40) \\ & 0 \leq v_{dt} \leq P_{dt}, \qquad \qquad d \in \Omega_D, t \in \Omega_T \ (41) \\ & 0 \leq v_{gt} \leq G_{gt}, \qquad \qquad g \in \Omega_G, t \in \Omega_T \ (42) \end{aligned}$$

B. Linearization of Natural Gas Network Constraints

The Weymouth equations presented in (27) are nonlinear and thus could not be readily solved by commercial MILP solvers. Authors in [7], [15] proposed to convert Weymouth equations with known gas flow directions into a set of linear constraints piecewise linear approximations. However, binary indicators would bring challenges for developing a tractable robust counterpart. Thus, convexification methods such as second order cone (SOC) relaxation [9], [21], [22] and Taylor series expansion [23] have been proposed. It is pointed out in [9], [22] that the SOC relaxation is generally inexact and may offer infeasible solutions. In turn, reference [22] presents a sequential SOCP algorithm to enhance solution feasibility. On the other hand, Taylor series expansion is applied to linearize Weymouth equation with positive flow direction in our previous work [23], while the solution quality and approximation accuracy are extensively studied. Since Taylor series expansion has high-quality approximation and its computation burden grows linearly with respect to the scale of the system, this paper adopts Taylor series expansion to linearize Weymouth equations.

To enhance tractability of nonlinear Weymouth equations and facilitate computation of the proposed distributionally robust optimization model, nonlinear gas flow equation (27) is reformulated as MILP constraints via Taylor series expansion. Based on our previous work, Weymouth equation with respect to a positive/negative flow direction can be linearized as constraints (43)-(46)/(47)-(50) [23], where $(\hat{\pi}_{s(p)t,n}^+, \hat{\pi}_{r(p)t,n}^+)$ is the nth predefined breakpoint. In turn, constraint (27) can be linearly approximated via (43)-(50) together with a limited number of binary variables f_{nl}^+/f_{nt}^- indicating gas flow directions.

$$G_{pt} \leq K_p \cdot \hat{v}_{pt,n}^+ \cdot \pi_{s(p)t} - K_p \cdot \hat{\phi}_{pt,n}^+ \cdot \pi_{r(p)t} + \left(1 - f_{pt}^+\right) \cdot M \tag{43}$$

$$\pi_{r(p)t} \leq \pi_{s(p)t} + \left(1 - f_{pt}^{+}\right) \cdot M \tag{44}$$

$$\pi_{r(p)t} \leq \pi_{s(p)t} + \left(1 - f_{pt}^{+}\right) \cdot M$$

$$\hat{v}_{pt,n}^{+} = \hat{\pi}_{s(p)t,n}^{+} / \sqrt{\left(\hat{\pi}_{s(p)t,n}^{+}\right)^{2} - \left(\hat{\pi}_{r(p)t,n}^{+}\right)^{2}}$$
(45)

$$\hat{\phi}_{pt,n}^{+} = \hat{\pi}_{r(p)t,n}^{+} / \sqrt{\left(\hat{\pi}_{s(p)t,n}^{+}\right)^{2} - \left(\hat{\pi}_{r(p)t,n}^{+}\right)^{2}}$$
(46)

$$-G_{pt} \leq K_p \cdot \widehat{v}_{pt,n} \cdot \pi_{r(p)t} - K_p \cdot \widehat{\phi}_{pt,n} \cdot \pi_{s(p)t} + \left(1 - f_{pt}\right) \cdot M \tag{47}$$

$$\pi_{s(p)t} < \pi_{r(p)t} + \left(1 - f_{pt}\right) \cdot M \tag{48}$$

$$\pi_{s(p)t} < \pi_{r(p)t} + \left(1 - f_{pt}\right) \cdot M$$

$$\hat{v}_{pt,n} = \hat{\pi}_{r(p)t,n} / \sqrt{\left(\hat{\pi}_{r(p)t,n}\right)^2 - \left(\hat{\pi}_{s(p)t,n}\right)^2}$$
(48)

$$\hat{\phi}_{pt,n} = \hat{\pi}_{s(p)t,n} / \sqrt{\left(\hat{\pi}_{r(p)t,n}\right)^2 - \left(\hat{\pi}_{s(p)t,n}\right)^2}$$
(50)

C. Abstract Formulation

The deterministic model could be written in a general abstract form as shown in (51)-(54). Binary vector \mathbf{x} refers to startup/ shutdown actions, on/off indicators, and gas flow direction indicators. All continuous variables are denoted as vector \mathbf{v} , representing dispatches of the IGES. Vector v represents electricity and natural gas load shedding. Equation (52) restricts x as binary variables. Constraints with only binary variables are represented as in (53). Operation conditions associated with both binary and continues variables are shown in (54).

$$\min_{\mathbf{x}, \mathbf{y}, \mathbf{v}} \mathbf{c}_{b}^{\mathsf{T}} \mathbf{x} + \mathbf{c}_{g}^{\mathsf{T}} \mathbf{y} + \mathbf{s}^{\mathsf{T}} \mathbf{v} \tag{51}$$

s.t.
$$\mathbf{x} \in \{0,1\}$$
 (52)

$$Ax \leq c_I$$
 (53)

$$Cx + Dy + Ev \le h \tag{54}$$

where A, C, D, E, c_b , c_g , c_l , s, and h are abstract matrices and vectors, representing coefficients of costs and constraints.

III. DISTRIBUTIONALLY ROBUST SCHEDULING MODEL

A two-stage distributionally robust model is proposed to study day-ahead coordinated scheduling of the IGES under uncertainties. Specifically, the IGES is designed to operate under the base-case condition with respect to electricity and gas load forecasts in the day-ahead timeframe, while adaptively and securely redispatching generating units, gas suppliers, and gas compressors in response to uncertainties in real time.

The following assumptions are adopted to facilitate modeling of the two-stage distributionally robust scheduling problem.

- 1) Unit commitment statuses are first stage variables and they remain unchanged in real-time dispatches [12], [21]. This is recognized by the fact that physical characteristics of most generating units restrict them from quickly changing their unit commitment statuses under uncertainties.
- 2) Similarly, gas flow directions are also regarded as first stage variables. Reversing gas flows would require complicated changes in operation statuses of overpressure protection devices. control valves, and compressor stations [22]. In turn, reversing gas flow directions is only allowed in the day-ahead framework with sufficient time and appropriate management.
- 3) As constraints (16)-(17) and (33)-(34) suggest that DR loads have minimum on/off time limits [4], [15], statuses of DRs are treated as first-stage variables and will not be changed in real time.
- 4) Fixed DR participation levels α_{dt} and α_{gt} are considered [4], [15]. Thus, in the proposed model, uncertainties of integrated gas-electricity DRs are reflected via the total amount of available DRs which varies with different realizations of total electricity and natural gas loads, while price uncertainties of individual segments in the demand response curves are not included. Alternatively, uncertain DR curves, such as those adopted in [23], could be integrated in the proposed model while the solution approach remains valid. Indeed, modeling uncertain DR curve in robust optimization is difficult and could complicate the solution algorithms. To this end, stochastic optimization approaches might have certain advantages by modeling uncertain demand response curve via multiple scenarios.

A. The Proposed Distributionally Robust Scheduling Model

In literature, stochastic programming and robust optimization have attracted much attention for their advantages in handling uncertainties. Stochastic programming seeks to optimize the expected value over a set of predefined scenarios, which requires the distribution probability of uncertain variables. By contrast, robust optimization tends to optimize the value over the worst-case situation within the predefined uncertainty set, where distribution probability of uncertain variables is not necessary. By leveraging the advantages of stochastic programming and robust optimization, distributionally robust optimization protects systems against the worst-case probability distribution in the ambiguity set with partial distributional information. The merit of distributionally robust optimization is that partial distributional information in stochastic programming is utilized to mitigate over-conservativeness of traditional robust optimization approach.

Recently, distributionally robust approaches have been applied in power systems to solve unit commitment problems with uncertain renewable generations and electrical loads. As an intermediate approach between stochastic programming and robust optimization, certain distribution information could be included to leverage advantages of the both methods [17]-[20]. In [17]-[18], a data-driven risk-averse stochastic unit commitment model is proposed where risk aversion stems from the worst-case probability distribution of renewable generation. The proposed model constructs a confidence set for distributions of uncertain parameters via historical data, and is solved via Benders decomposition. In addition, references [19]-[20] adopt ambiguity set with moment-based information to partially capture the distributional information while addressing the computational issue via affine decision rules. Moreover, the formulations in [17]-[20] optimize the first-stage unit commitment cost and second-stage worst-case expected dispatch cost. Differently, the basic idea of the proposed model is to find a base-case scheduling solution (including both unit commitment and dispatch) with respect to the optimal base-case system social welfare and worst-case expected load shedding cost over an ambiguity set. Compared with traditional distributionally robust models which optimize the worst-case expected system social welfare, the proposed model has two major advantages: (i) Less conservativeness. The proposed model is less conservative because it optimizes the base-case system social welfare while considering the worst-case expected load shedding cost; (ii) Practical applications. Instead of only providing unit commitment and gas flow direction solutions, the proposed model also derives base-case dispatch solutions that could be directly used by Independent System Operators (ISOs), Regional Transmission Organizations (RTOs), and Natural Gas System Operators for the day-ahead market clearing.

The distributionally robust scheduling model is presented in (55), where load shedding is not allowed in the base case.

(55), where load shedding is not allowed in the base case.

$$\min_{x,y^b} c_b^T x + c_g^T y^b + \sup_{\mathbb{P} \in \mathcal{D}} \mathbb{E}_{\mathbb{P}} \{ L(x, y^b, \xi) \}$$
s.t. $\mathbf{x} \in \{0,1\}$

$$A\mathbf{x} \leq c_l$$

$$C\mathbf{x} + D\mathbf{y}^b \leq \mathbf{h}$$
where $\mathbb{E}_{\mathbb{P}} \{ L(x, y^b, \xi) \}$ denotes the expected value with respect to

where $\mathbb{E}_{\mathbb{P}}\{L(x,y^o,\xi)\}$ denotes the expected value with respect to the distribution \mathbb{P} of uncertainty variables ξ ; \mathcal{D} is the ambiguity

set; y^b represents the first-stage base-case dispatch decisions corresponding to forecasted electricity and gas loads; the second-stage dispatch problem under uncertainties is expressed as in (56).

$$L(x,y^{b},\xi) = \min_{y,v} s^{T} v$$

s.t.
$$Cx+Dy+Ev \le h(\xi);$$

 $Fy^b+Gy \le \Delta$ (56)

where y denotes the second-stage dispatch decisions in response to uncertainties; C, D, E, F, G, s, and Δ are abstract matrices and vectors; the second set of constraints describes that redispatches of generating units and gas suppliers are limited by their corrective ramping capabilities [12], [21]; the right-hand side vector $h(\xi)$ of the first set of constraints is affinely affected by uncertainties, which can be commonly expressed as follows:

$$h(\xi) = h^0 + \sum_{w} h_{w}^{\xi} \xi_{w} \tag{57}$$

where w is index of uncertainty parameters; h^0 denotes constant term free from uncertainties; h_w^{ξ} represents coefficient of the affine dependence on the wth uncertainty parameter ξ_w .

It is noted that equations (43)-(50) representing linearized Weymouth equation only include binary variables related to gas flow directions. Thus, after gas flow directions are determined in the first stage of the distributionally robust optimization problem, the second-stage problem of the proposed model does not contain any binary variables. Indeed, this is the advantage of applying Taylor series expansion to linearize Weymouth equation, which could facilitate the solution via distributionally robust optimization.

B. Ambiguity Set

The ambiguity set includes a family of probability distributions that have common statistical properties. A general formulation of the ambiguity set is given in (58) [20], [].

$$\mathcal{D} = \left\{ \mathbb{P} \in \mathcal{P}_0(\mathbb{R}^W) \middle| \begin{array}{c} \mathbb{P}\{\xi \in \Xi\} = 1 \\ \mathbb{E}_{\mathbb{P}}\{\xi\} = \mu \\ \mathbb{E}_{\mathbb{P}}\{z_o(\xi)\} \le \gamma_o, \quad o = 1, 2, \dots O \end{array} \right\}$$
 (58)

where $\mathcal{P}_0(\mathbb{R}^W)$ denotes the set of all probability distributions on \mathbb{R}^W and W is number of uncertainty parameters. The first constraint ensures that all outcomes of ξ are within the support set Ξ . The second line suggests that the expectation of ξ is μ . The third constraint describes moment information of uncertainties via function $z_o(\bullet)$, restricting that the generalized moment cannot exceed a predefined threshold γ_o . By introducing an O-dimension auxiliary vector φ , the ambiguity set \mathcal{D} could be reformulated as the projection of an extended ambiguity set $\overline{\mathcal{D}}$ (59).

$$\overline{\mathcal{D}} = \left\{ \mathbb{Q} \in \mathcal{P}_0(\mathbb{R}^W \times \mathbb{R}^O) \middle| \begin{array}{l} \mathbb{P}\{(\xi, \varphi) \in \overline{\Xi}\} = 1 \\ \mathbb{E}_{\mathbb{Q}}\{\xi\} = \mu \\ \mathbb{E}_{\mathbb{Q}}\{\varphi\} \le \gamma \end{array} \right\}$$
(59)

where the uncertainty domain is also extended to a lifted support set as in (60).

$$\overline{\Xi} = \left\{ (\xi, \varphi) \middle| \begin{array}{l} \xi \in \Xi \\ z_o(\xi) \le \varphi_o \le \max z_o(\xi), o = 1, 2, \dots O \end{array} \right\}$$
 (60)

Similar to the uncertainty set of robust optimizations, the support set Ξ adopts lower and upper bounds to limit each uncertainty parameter ξ_w (61).

$$\mathbf{\Xi} = \left\{ \boldsymbol{\xi} \mid \boldsymbol{\xi}_{w}^{\min} \leq \boldsymbol{\xi}_{w} \leq \boldsymbol{\xi}_{w}^{\max}, \quad w = 1, 2, \dots W \right\}$$
 (61)

As for the function $z_o(\bullet)$, this paper adopts the following piecewise linear formulation (62), which allows us to derive a computationally tractable equivalent robust counterpart as an MILP problem [20], [24]-[25]. Although there are other nonlinear choices of functions $z_o(\bullet)$ to characterize variances or higher-order moment information, the associated computational

burden for complicated operation problems on large-scale systems could be overwhelming. Instead, piecewise linear function (62) has some exclusive advantages: (i) The first-order deviation information is included, while correlations between uncertain variables are partially reflected, and (ii) More importantly, a computational tractable equivalent robust counterpart could be derived.

$$z_o(\xi) = \max\{g_o^T \xi - q_o, 0\}, o = 1, 2, \dots O$$
 (62)

where \mathbf{g}_o is projection direction of the first-order deviation in $\boldsymbol{\xi}$, and q_0 is the cut-off constant. In other words, the second constraint of expression (60) would suggest that the positive part of $\mathbf{g}_{0}^{T}\boldsymbol{\xi}$ - q_{0} should be no larger than φ_{0} . Reference [25] presented a two-step data-based strategy to determine parameters of equation (62) in the proposed model. Principal component analysis (PCA) is applied to capture correlation information between uncertain variables, and all dominant statistical information could be reflected in the projection directions \mathbf{g}_{o} , truncation point q_{o} , and parameter γ_{o} . In addition, with a chosen function $z_o(\xi)$, max $z_o(\xi)$ in (60) represents a constant which could be calculated as the largest value of $z_o(\xi)$ over historical data.

With the support set Ξ and linear moment function respectively defined in (61) and (62), the lifted support set can be reformulated via a set of linear inequality constraints (63), which could be further written in a compact matrix form (64).

$$\overline{\Xi} = \left\{ (\xi, \varphi) \middle| \begin{array}{c} \xi \leq \xi^{\max} \\ -\xi \leq -\xi^{\min} \\ 0 \leq \varphi_o, o = 1, 2, \dots O \\ g_o^T \xi - q_o \leq \varphi_o \leq \max(g_o^T \xi - q_o), o = 1, 2, \dots O \end{array} \right\}$$
(63)

$$\overline{\Xi} = \{ (\xi, \varphi) \mid H\xi + I\varphi \leq c_w \}$$
(64)

IV. SOLUTION METHODOLOGY

This section discusses an affine decision rule-based method to effectively solve the proposed two-stage distributionally robust model, followed by the calculation of LMEPs/LMGPs.

A. Reformulation of the Worst-Case Expectation Problem

The inner maximization problem $\sup_{\mathbb{Q} \in \overline{\mathcal{D}}} \mathbb{E}_{\mathbb{Q}} \{ L(x, y^b, \xi) \}$ in (55)

introduces significant computational burden due to the infinite dimensions of probability measure Q. Typically, the inner problem can be dualized to transform into a minimization problem to facilitate the computation.

The explicit expression of the inner worst-case expectation problem is shown in (65).

$$\sup_{\mathbb{Q}\in\mathcal{D}}\int_{\Xi} p(\xi,\varphi) L(x,y^{b},\xi) d\xi d\varphi$$

s.t. $\int_{\Xi} p(\xi, \varphi) d\xi d\varphi = 1:(\eta)$

$$\int_{\Xi} p(\xi, \varphi) \, \xi \, d\xi \, d\varphi = \mu : (\rho)$$

$$\int_{\Xi} p(\xi, \varphi) \varphi \, d\xi \, d\varphi \leq \gamma : (\beta) \tag{65}$$

where joint probability density function $p(\xi, \varphi)$ is the decision variable; symbols in the parenthesis at the end of constraints are dual variables of corresponding constraints.

The equivalent dual problem of (65) is formulated as in (66) [20], [24]-[25]. It could be observed that the last constraint is a robust constraint against uncertainty set $\overline{\Xi}$.

$$\min_{\eta,\rho,\beta} \eta + \mu^{\mathsf{T}} \rho + \gamma^{\mathsf{T}} \beta
\text{s.t. } \beta \ge 0
\eta + \xi^{\mathsf{T}} \rho + \varphi^{\mathsf{T}} \beta \ge L(x, y^{\mathsf{b}}, \xi), \quad \forall (\xi, \varphi) \in \overline{\Xi}$$
(66)

B. Reformulation of the Proposed Two-Stage Distributionally Robust Problem

The proposed two-stage distributionally robust model is generally intractable and NP-hard, because calculating the worst-case expectation involves enumerating all realizations within the lifted support set Ξ . One practical approach is to employ the affine decision rule (ADR) [24]-[26], which restricts that the recourse decisions are affinely dependent on uncertainty parameters as in (67)-(68).

$$y_a(\xi, \varphi) = y_a^0 + \sum_u y_{\underline{a}w}^{\xi} \xi_w + \sum_o y_{\underline{a}o}^{\varphi} \varphi_o$$
 (67)

$$v_a(\boldsymbol{\xi}, \boldsymbol{\varphi}) = v_a^0 + \sum_w v_{aw}^{\boldsymbol{\xi}} \boldsymbol{\xi}_w + \sum_o v_{ao}^{\boldsymbol{\varphi}} \boldsymbol{\varphi}_o \tag{68}$$

 $v_a(\xi, \varphi) = v_a^0 + \sum_w v_{aw}^{\xi} \xi_w + \sum_o v_{ao}^{\varphi} \varphi_o$ where a is index of recourse variables; y_a^0 and v_a^0 denote constants; $y^{\xi}_{aw}, y^{\varphi}_{ao}, v^{\xi}_{aw}$, and v^{φ}_{ao} are coefficients associated with uncertainty parameters ξ_w and auxiliary variables φ_o .

Recently, ADR has been adopted to solve the multi-stage distributionally robust problems. By dualizing the inner maximization as discussed in Section IV.A, the proposed two-stage distributionally robust problem could be equivalently recast into an equivalent robust optimization problem in (69)-(76).

$$\min \mathbf{c}_{b}^{\mathrm{T}} \mathbf{x} + \mathbf{c}_{\rho}^{\mathrm{T}} \mathbf{y}^{\mathrm{b}} + \eta + \boldsymbol{\mu}^{\mathrm{T}} \boldsymbol{\rho} + \boldsymbol{\gamma}^{\mathrm{T}} \boldsymbol{\beta}$$
 (69)

s.t.
$$\beta \geq 0$$
 (70)

$$x \in \{0,1\} \tag{71}$$

$$Ax \leq c_I$$
 (72)

$$Cx + Dy^b \le h \tag{73}$$

$$\eta + \xi^{\mathsf{T}} \rho + \varphi^{\mathsf{T}} \beta \geq s^{\mathsf{T}} \nu(\xi, \varphi), \qquad \forall (\xi, \varphi) \in \overline{\Xi} : (\lambda)$$
 (74)

$$Cx+Dy(\xi,\varphi)+Ev(\xi,\varphi)\leq h(\xi), \ \forall (\xi,\varphi)\in \overline{\Xi}:(\sigma)$$
 (75)

$$Fy^b + Gy(\xi, \varphi) \leq \Lambda, \qquad \forall (\xi, \varphi) \in \overline{\Xi}:(\delta)$$
 (76)

The last three constraints (73)-(75) are classical robust constraints on the polytopic uncertainty set $\overline{\Xi}$. Methods from existing literatures could be adopted to convert these three infinite-dimensional constraints into their robust counterparts [20], [26], [27].

We take the first uncertain linear constraint (74) as an example to show the details for deriving the MILP-based deterministic counterpart. Constraint (74) can be reformulated as the following worst-case form (77).

$$\min_{(\vec{\xi}, \boldsymbol{\theta}) \in \Xi} \left\{ \eta + \boldsymbol{\xi}^{\mathrm{T}} \boldsymbol{\rho} + \boldsymbol{\varphi}^{\mathrm{T}} \boldsymbol{\beta} - \boldsymbol{s}^{\mathrm{T}} \boldsymbol{v}(\boldsymbol{\xi}, \boldsymbol{\varphi}) \right\} \ge 0 \tag{77}$$

The worst-case expression (77) could be further written in an explicit formulation (78).

$$\min_{(\xi,\varphi)\in\Xi} \left\{ \eta + \sum_{w} \xi_{w} \rho_{w} + \sum_{o} \varphi_{o} \beta_{o} - \sum_{a} s_{a} v_{a}^{0} - \sum_{a} \sum_{w} s_{a} v_{aw}^{\xi} \xi_{w} - \sum_{a} \sum_{o} s_{a} v_{ao}^{\varphi} \varphi_{o} \right\} \ge 0 \quad (78)$$

Note that the lifted support set $\overline{\Xi}$ is defined in (63). By taking the dual of the minimization formulation (78), equivalent MILP-based constraints of uncertain linear constraint (74) is derived as in (79)-(82).

$$\eta - \mathbf{s}^{\mathrm{T}} \mathbf{v}^{0} - \lambda^{\mathrm{T}} \mathbf{c}_{\mathbf{w}} \ge 0 \tag{79}$$

$$\lambda \geq 0$$
 (80)

$$\lambda^{\mathrm{T}} \boldsymbol{H}_{w} = \sum_{a} s_{a} v_{aw}^{\xi} - \rho_{w}, \qquad w = 1, 2, \dots W$$
 (81)

$$\lambda^{\mathsf{T}} I_o = \sum_a s_a v_{ao}^{\varphi} - \beta_o, \qquad o = 1, 2, \dots O$$
 (82)

where H_w is the wth column of matrix H and I_o is the oth

column of matrix I.

Finally, the proposed two-stage distributionally robust problem is reformulated as an MILP-based deterministic optimization problem (83). As pointed out and proved in [25], employing affine decision rule would provide a feasible yet conservative solution. Since affine decision rule is only applied to approximate worst-case expected load shedding cost, the base-case dispatch decisions obtained is of high-quality.

where r and u are indices of constraints; h_{rw}^{ξ} is the rth element of vector \boldsymbol{h}_{w}^{ξ} ; Row vectors \boldsymbol{C}_{r}^{T} , \boldsymbol{D}_{r}^{T} , and \boldsymbol{E}_{r}^{T} denote the rth rows of matrices \boldsymbol{C}^{T} , \boldsymbol{D}^{T} , and \boldsymbol{E}^{T} respectively; Row vectors \boldsymbol{F}_{u}^{T} and \boldsymbol{G}_{u}^{T} denote the uth rows of matrices \boldsymbol{F}^{T} and \boldsymbol{G}^{T} .

C. Calculation of Locational Marginal Electricity/Gas Prices

When electricity/natural gas transmission network congestions occur, the electricity/natural gas market cannot be cleared at the system level. Instead, the market will be cleared at the bus/node level. Similar to the concept of LMP in electricity market, LMGP is defined as the cost of supplying the next kcf/h of gas load at a certain location, considering costs of gas production and transmission [3], [28]. A bilateral gas-electricity market is proposed in [29] where the two markets trade energy at locational marginal prices.

The calculation of locational marginal electricity/gas prices involves two steps. (i) Solve problem (83) to obtain unit commitment (UC) statuses, gas flow directions, and dispatch results; (ii) The optimal base-case solutions of problem (83) is used to calculate LMEPs/LMGPs. Specifically, problem (51)-(54) is solved with determined UC results \hat{I}_{it} , gas flow directions $\hat{f}_{pt}^+/\hat{f}_{pt}^-$, and optimal dispatch solutions $\hat{P}_{it}/\hat{P}_{dt}/\hat{G}_{jt}/\hat{G}_{gt}$ while considering constraints (84)-(87) to derive true marginal electricity/gas prices, where ΔP_{it}^\pm , ΔP_{dt}^\pm , ΔG_{jt}^\pm , and ΔG_{gt}^\pm are small deviations to calculate LMEPs/LMGPs. Dual variables obtained from constraint (6) are LMEPs, and dual variables of constraint (24) are regarded as LMGPs.

$$\widehat{P}_{it} - \Delta P_{it} \leq P_{it} \leq \widehat{P}_{it} + \Delta P_{it}^{+} \tag{84}$$

$$\widehat{P}_{dt} - \Delta P_{dt} \le P_{dt} \le \widehat{P}_{dt} + \Delta P_{dt}^{+} \tag{85}$$

$$\widehat{G}_{jt}^{-} \Delta G_{jt}^{-} \leq \widehat{G}_{jt} + \Delta G_{jt}^{+}$$
(86)

$$\widehat{G}_{gt} - \Delta G_{gt}^{-} \le G_{gt} \le \widehat{G}_{gt} + \Delta G_{gt}^{+} \tag{87}$$

V. CASE STUDIES

A 6-bus power system/7-node natural gas system and the modified IEEE 118-bus power system/12-node natural gas system are used to demonstrate the proposed distributionally robust scheduling model, for analyzing the impact of an effective deployment of integrated gas-electricity DRs on market clearing and LMEPs/LMGPs. Electricity load shedding costs is set as 1000 \$/MWh, and gas load shedding cost is 1207 \$/kcf (e.g. 4000\$/MWh) suggesting a higher priority of natural gas residential loads. Detailed data of the test systems can be found in [30]. The small deviations in equations (84)-(87) need to be carefully chosen to derive true marginal electricity/gas prices. In the case studies of the paper, these small deviations are set in the range of [10⁻⁵, 10⁻²].

A. 6-Bus Power System/7-Node Natural Gas System

The 6-bus power system/7-node natural gas system shown in Fig. 2 is studied for a two-hour period to illustrate effectiveness of the proposed distributionally robust scheduling model. Electricity/gas loads at all buses/nodes are assumed eligible to provide DR. Minimum on/off time limits of generators and integrated gas-electricity DRs are both set as 1, and ramping constraints are ignored for simplicity. Generators G1 and G2 are initially on.

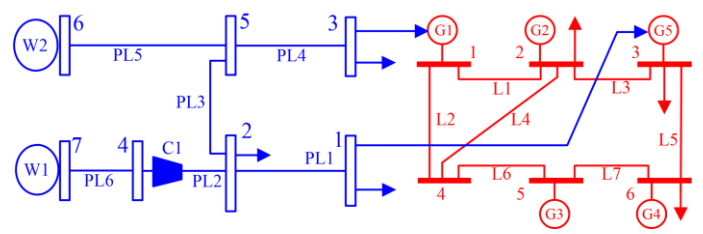


Fig. 2 6-bus power system/7-node natural gas system.

The following five cases are studied to illustrate the impacts of distributionally robust scheduling and integrated gas-electricity DR.

- Case 1: Deterministic scheduling without integrated gas-electricity DR.
- Case 2: Integrated gas-electricity DR is applied after unit commitment decisions and gas flow directions have been settled in Case 1.
- Case 3: Case 1 with integrated gas-electricity DR.
- Case 4: Case 1 with distributionally robust scheduling.
- Case 5: Case 4 with integrated gas-electricity DR.

Case 1: This is the base case. First, approximation accuracy of Taylor series expansion is studied. The method proposed in Section III.C of reference [23] is used to examine the errors of Weymouth equation approximation with different numbers of breakpoints in equations (43)-(50). The results are shown in Fig. 3. As it is observed, gas network is not congested at hour 1, so the maximum relative errors are extremely small regardless the number of breakpoints, indicating that the obtained solution is feasible and optimal to the original Weymouth equation. At hour 2, gas network congestions occur with increased load, and the maximum relative errors of Weymouth equation approximation decrease with the increase in the number of breakpoints. When the number of breakpoints is larger than 150, the maximum relative error is smaller than 10-4, which suggests that the original Weymouth equation is approximated with high

quality. In addition, the impact of Taylor series expansion on LMEPs/LMGPs are tested. Fig. 4 shows LMGPs against different numbers of breakpoints at hour 2, since LMEPs are not influenced. It is observed that when no breakpoints are considered, LMGPs of all nodes are the same, indicating that no congestion occurs in the gas network. On the other hand, by gradually adding breakpoints, both gas network congestion and difference in LMGPs emerge. It could also be seen that when the number of breakpoints reaches 150, the changes in LMGPs become negligible. It is concluded that a proper number of breakpoints can reasonably enhance approximation accuracy of the Taylor series expansion, and 150 is an appropriate number of breakpoints for this test system.

Table I summarizes results of Case 1. At off-peak hour 1, base units G1 and G2 are sufficient to cover electricity loads. However, at peak hour 2, four units are turned on to supply electricity loads. Due to congestion of line L3, higher LMEPs are encountered at buses 3 and 6. For natural gas system, network congestion has limited the production of gas supplier 1 with cheaper cost, and G1 is not operated at full capacity. In turn, a much higher LMGP is found at node 3. The energy payment of DR loads is \$86,199.29, calculated as the multiplication of energy consumptions and corresponding LMEPs/LMGPs at individual hours.

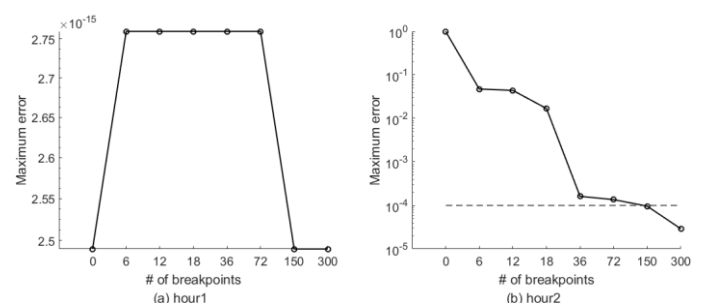


Fig. 3 Maximum error of Weymouth equation via Taylor series expansion.

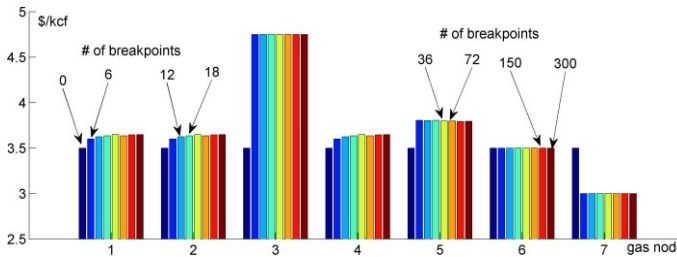


Fig. 4 Sensitivity analysis of Taylor series expansion in calculating LMGPs.

TABLE I RESULTS OF CASE 1-3							
		Case 1		Case 2		Case 3	
		Hour 1	Hour 2	Hour 1	Hour 2	Hour 1	Hour 2
# of Comm	itted units	2	4	2	4	2	3
	Bus 1	37.46	61.51	38.86	56.24	39.65	58.05
	Bus 2	37.46	58.88	38.86	56.24	39.65	58.05
LMEP	Bus 3	37.46	83.27	38.86	56.24	39.65	58.05
(\$/MWh)	Bus 4	37.46	62.65	38.86	56.24	39.65	58.05
	Bus 5	37.46	66.47	38.86	56.24	39.65	58.05
	Bus 6	37.46	79.60	38.86	56.24	39.65	58.05
	Node 1	3.00	3.65	3.00	3.36	3.02	3.37
	Node 2	3.00	3.65	3.00	3.36	3.02	3.37
LMGP (\$/kcf)	Node 3	3.00	4.75	3.00	3.81	3.06	3.82
	Node 4	3.00	3.65	3.00	3.36	3.02	3.37
	Node 5	3.00	3.79	3.00	3.50	3.04	3.50
	Node 6	3.00	3.50	3.00	3.50	3.04	3.50
	Node 7	3.00	3.00	3.00	3.00	3.02	3.37
Production cost (\$)		68,588.04		66,104.62		65,228.35	
DR payment (\$)		86,199.29		70,492.75		71,485.17	

Case 2: The minimum bidding prices of electricity and gas DR loads are set as 37 \$/MWh and 3 \$/kcf, while their maximum bidding prices are respectively set as 84 \$/MWh and 4.8 \$/kcf. E_d^{max} and E_g^{max} are set as 0, indicating that the curtailed load at certain time periods is fully shifted to other time periods. DR participation levels α_{dt} and α_{gt} are set as 0.2, while the entire range of DR load level is evenly divided into five segments.

Results of Case 2 are shown in Table I. In this case, a portion of electricity/gas loads is shifted from hour 2 to hour 1 to maximize system social welfare. Since four units are committed at hour 2, only 56MW of electricity DR is shifted from peak hour to off-peak and 1144.75 kcf/h of gas DR is shifted. Due to the reduction in gas load at hour 2, G1 receives sufficient gas supply to operate at its full capacity. In turn, much lower LMEPs/LMGPs are observed at peak hour. The energy production cost is decreased from \$68,588.04 in Case 1 to \$66,104.62. The DR load payment is reduced to \$70,492.75.

Case 3: Different from Case 2, this case introduces integrated gas-electricity DR into the scheduling model to seek more economical scheduling decisions. Table I compares results of Case 3 with those of Cases 1-2. In this case, 75 MW of electricity DR is shifted from peak hour to off-peak. Consequently, only three generating units are committed at hour 2 for economic operations. As the output of generator G1 in this case is increased to 225 MW from 206 MW in Case 2, which consumes more natural gas at hour 1, only 864.6 kcf/h of gas DR is shifted from hour 2 to hour 1. As compared to Case 1, the savings of energy production cost in this case increases to 4.90% from 3.62% in Case 2. Thus, integrating electricity/gas DR resources could derive more efficient scheduling decisions in terms of higher system social welfare. However, LMEPs/ LMGPs are slightly increased as compared to Case 2, which leads to the increase in DR loads' payment. That is, when deploying DRs with the objective of maximizing system social welfare, LMEPs/LMGPs at certain buses/nodes may increase and consumers may encounter more payments.

To further comprehensively test the effect of electricity/gas DR on the IGES and LMEPs/LMGPs, the following five additional cases are carried out.

Case 3.1: Case 1 with only electricity DR.

Case 3.2: Case 1 with only gas DR.

Case 3.3: Case 1 with electricity load at bus 2 increased by 300% and gas load at node 3 increased by 50%.

Case 3.4: Case 3.3 with electricity DR.

Case 3.5: Case 3.3 with gas DR.

Results of Cases 3.1-3.2 at peak hour 2 are shown in Table II. As compared to Case 1, when electricity DR is considered in Case 3.1, both LMEPs and LMGPs at hour 2 are decreased. In this case, electricity transmission line L3 is not congested anymore, where LMEPs at all buses are the same. On the other hand, when natural gas DR is introduced in Case 3.2, output of G1 is increased from 242.9 MW in Case 1 to its maximum capacity 250MW which helps bring down LMEPs slightly. Cases 3.3-3.5 are used to simulate severe weather conditions with significantly high electricity and gas consumptions, and results of these cases are shown in Table III. Due to higher priority of residential gas loads, the IGES would reduce gas consumptions of gas-fired units to avoid residential gas load shedding. As pipeline PL4 reaches its transmission capacity in

Case 3.3, higher priority of residential gas load has limited the gas supply to gas-fired units, leading to 75.46MWh of electricity load shedding. When electricity DR is considered in Case 3.4, a portion of electricity loads is shifted from peak hour to off-peak hour to avoid electricity load shedding, and more natural gas is utilized by gas-fired units G1 and G5. In Case 3.5, introducing gas DR could also mitigate electricity load shedding and reduce the number of online units.

From these cases, it could be concluded that, electricity DR could help reduce LMGPs by alleviating gas network congestions. Analogously, natural gas DR could also be applied to relieve electricity shortages in peak hours by securing the supply of natural gas to gas-fired units.

TABLE II RESULTS OF CASES 3.1-3.2 AT HOUR 2

		Case 3.1	Case 3.2			Case 3.1	Case 3.2
	Bus 1	57.26	61.02		Node 1	3.56	3.36
	Bus 2	57.26	58.88		Node 2	3.56	3.36
LMEP	Bus 3	57.26	78.75	LMCD	Node 3	4.42	3.81
(\$/MWh)	Bus 4	57.26	61.95	LMGP (\$/kcf)	Node 4	3.56	3.36
	Bus 5	57.26	65.07		Node 5	3.68	3.50
	Bus 6	57.26	75.76		Node 6	3.50	3.50
# of Committed units		3	4		Node 7	3.00	3.00

TABLE III COMPARISON OF	RESULTS IN	CASES 3.3-3.5
-------------------------	------------	---------------

	Electricity load	Total gas consumption	# of Comm	itted units
	shedding (MWh)	of G1 and G5 (kcf)	Hour 1	Hour 2
Case 3.3	75.46	5482.38	3	5
Case 3.4	0	6746.08	3	5
Case 3.5	0	6453.10	2	5

Case 4: in this case, uncertainties of electricity and natural gas loads are considered via distributionally robust scheduling. Variations of electricity and gas loads are set as 10% of their forecast values while the expectations of variations μ are set as 0. Projection directions g are set as 1, and values of q are set as 0. Generalized moment thresholds γ are 40% of electricity and gas load deviations. With these settings, for the electricity network, the first-moment constraints in (58) restrict that the expectation of the positive part of electricity load deviations should be no larger than γ . Obtaining this statistical information from historical data is rather straightforward, by just calculating the expectation of the positive part of deviations from historical load data.

The proposed distributionally robust scheduling model optimizes the base-case social welfare and worst-case expected load shedding cost, while adaptively adjusting generation dispatches in response to uncertainties in real time. The results are shown in Table IV, where penalty cost represents worst-case expected load shedding cost. As compared to Case 1, all five units are committed at hour 2 to ensure operational security of power system and avoid high load shedding cost. It is also observed that with more units committed, G4 can operate at a lower cost and LMEPs/LMGPs are slightly smaller than Case 1.

Case 5: when DR is introduced in this case, the production cost and DR loads' payment are considerably decreased as compared to Case 4. Compared with Case 3, distributionally robust model by scheduling enough reserves could avoid potential transmission line congestions and reduce LMEPs. Although the production cost is slightly increased by committing more units, the IGES could operate more securely against uncertainties and energy consumers may benefit from a lower payment. Furthermore, two additional cases, Cases

5.1-5.2 with the load shedding costs decreased to 10% and 1% of their original values, are studied to explore the impact of load shedding cost. The results are shown in Table IV. When load shedding cost reduces, load shedding emerges under uncertainties to achieve higher social welfare. That is, the production cost is reduced to \$65,228.35 by only committing three units at peak hour, at the expense of a small amount of worst-case expected load shedding penalty cost.

	T. IDEE I	V KLBOLIB O			
		Case 4	Case 5	Case 5.1	Case 5.2
# of Commi	tted units	5	4	3	3
	Bus 1	61.02	56.24	58.05	58.05
	Bus 2	58.88	56.24	58.05	58.05
LMEP	Bus 3	78.75	56.24	58.05	58.05
(\$/MWh)	Bus 4	61.95	56.24	58.05	58.05
	Bus 5	65.07	56.24	58.05	58.05
	Bus 6	75.76	56.24	58.05	58.05
	Node 1	3.64	3.36	3.37	3.37
	Node 2	3.64	3.36	3.37	3.37
LMGP	Node 3	4.71	3.81	3.82	3.82
	Node 4	3.64	3.36	3.37	3.37
(\$/kcf)	Node 5	3.78	3.50	3.50	3.50
	Node 6	3.50	3.50	3.50	3.50
	Node 7	3.00	3.00	3.00	3.00
Production cost (\$)		69,353.70	66,104.62	65,228.35	65,228.35
Penalty cost (\$)		0	0	281.35	28.14
DR payment (\$)		84,616.75	70,492.75	71,485.17	71,485.17

In order to show how partial distributional information would affect the worst-case expected load shedding and decision making, sensitivity analysis with different values of predefined threshold γ in (59) is carried out. Load shedding costs are set as 10% of their original values, and the results are shown in Table IV. Because γ represents the expectation of the positive part of load deviations, larger γ would suggest larger variations. Particularly, when γ equals 0, zero penalty cost is obtained as no uncertainty is indicated in the ambiguity set. As it is observed in Table IV, worst-case expected load shedding penalty cost increases as γ increases, indicating that more loads are cut off. It is also noted that choosing different values of γ does not affect the number of committed units and the base-case production cost in this specific case.

TABLE IV WORST-CASE EXPECTED LOAD SHEDDING PENALTY COST AGAINST γ γ 0 10% 20% 40% 60%

Penalty cost (\$) 0 70.34 140.68 281.35 351.69

B. IEEE 118-Bus Power System/12-Node Gas System

A modified IEEE 118-bus power system together with a 12-node natural gas system is applied to further demonstrate scalability of the proposed approach. Peak values of electricity and gas loads are 6000MW and 18000kcf/h.

Fig. 5 shows the system scheduled electricity and gas load profiles with respect to different DR participation levels. Compared with the base case without DR, a large amount of electricity loads is shifted from peak hours 9-11 and 15-24 to off-peak hours 1-8, and a portion of gas loads is shifted from heavily loaded hours 9-20 to hours 1-8 and 21-24 to maximize system social welfare. With the increase in DR participation level, more loads are shifted to off-peak hours and the electricity/gas load profiles become much flatter. That is, the IGES makes fully utilization of all available DR capabilities, transmission network capabilities, and cheap energy production units/suppliers to maximize system social welfare. As a result,

the energy production cost is reduced from \$7,000,933 to \$6,912,039 with α =0.1 and \$6,904,838 with α =0.2.

When uncertainties are considered in the distributionally robust scheduling model, without integrated gas-electricity DR, 68 more unit hours are committed to provide enough reserves, and gas supplier 2 is operated at low capacity to offer ramping capabilities against upward uncertainties of gas loads. In turn, the energy production cost is increased to \$7,009,654. If integrated gas-electricity DR is further considered, lower production cost is achieved. In addition, production of cheaper gas supplier 2 is increased from 183,419 kcf to 203,832 kcf.

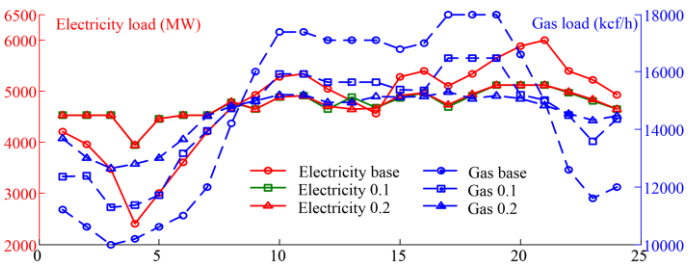


Fig. 5 Load profiles with respect to different DR participation levels.

VI. CONCLUSION

Integrated gas-electricity DR is one of the most important applications in the future interdependent electricity and natural gas systems, which could improve energy efficiency and increase system security. This paper proposes a distributionally robust scheduling model for the IGES while considering integrated gas-electricity DR. The proposed model optimizes base-case system social welfare and worst-case expected load shedding cost. The impact of integrated gas-electricity DR on market clearing and LMEPs/LMGPs is also studied.

Simulation results show that integrated gas-electricity DR could positively reduce energy production cost and LMEPs/LMGPs. In addition, incorporating gas DR can relieve electricity shortage of power system, while introducing electricity DR can mitigate natural gas network congestions. The proposed distributionally robust scheduling model with integrated gas-electricity DR incurs slightly higher operation cost to maintain system security against uncertainties of electricity and natural gas loads. In addition, the proposed model could also avoid potential transmission network congestions and benefit consumers with less energy payment.

REFERENCES

- [1] EIA, Annual Energy Outlook 2018, [Online]. Available: https://www.eia.gov/outlooks/aeo/pdf/AEO2018.pdf.
- [2] M. Shahidehpour, Y. Fu, and T. Wiedman, "Impact of natural gas infrastructure on electric power systems," *Proc. IEEE*, vol. 93, no. 5, pp. 1042-1056, May 2005.
- [3] L. Wu. "Impact of price-based demand response on market clearing and locational marginal prices," *IET Gener., Transm., Distrib.*, vol. 7, no. 10, pp. 1087-1095, Oct. 2013.
- [4] H. Wu, M. Shahidehpour, A. Alabdulwahab, and A. Abusorrah. "Thermal generation flexibility with ramping costs and hourly demand response in stochastic security-constrained scheduling of variable energy sources," *IEEE Trans. Power Syst.*, vol. 30, no. 6, pp. 2955-2964, Nov. 2015.
- [5] Whitehouse Introduces Innovative Natural Gas Demand Response Legislation, 2018, [Online]. Available: https://www.whitehouse.senate. gov/news/release/whitehouse-introduces-innovative-natural-gas-demand-response-legislation.
- [6] Demand Response for Natural Gas Distribution, 2018, [Online]. Available: http://files.brattle.com/files/13929_demand_response_for_

- natural_gas_distribution.pdf.
- [7] C. Correa-Posada and P. Sanchez-Martin, "Integrated power and natural gas model for energy adequacy in short-term operation," *IEEE Trans. Power Syst.*, vol. 30, no. 6, pp. 3347-3355, Nov. 2015.
- [8] A. Zlotnik, L. Roald, S. Backhaus, M. Chertkov, and G. Andersson, "Coordinated scheduling for interdependent electric power and natural gas infrastructures," *IEEE Trans. Power Syst.*, vol. 32, no. 1, pp. 600-610, Jan. 2017.
- [9] Y. He, M. Yan, M. Shahidehpour, Z. Li, C. Guo, L. Wu, and Y. Ding, "Decentralized optimization of multi-area electricity-natural gas flows based on cone reformulation," *IEEE Trans. Power Syst.*, vol. 33, no. 4, pp. 600-610. Jul. 2018.
- [10] A. Alabdulwahab, A. Abusorrah, X. Zhang, and M. Shahidehpour, "Coordination of interdependent natural gas and electricity infrastructures for firming the variability of wind energy in stochastic day-ahead scheduling," *IEEE Trans. Sustain. Energy*. vol. 6, no. 2, pp. 606-615. Apr. 2015
- [11] Z. Qiao, Q. Guo, H. Sun, Z. Pan, Y. Liu, and W. Xiong, "An interval gas flow analysis in natural gas and electricity coupled networks considering the uncertainty of wind power," *Appl. Energy*. vol. 201, pp. 343-353. Sept. 2015.
- [12] C. He, L. Wu, T. Liu, and M. Shahidehpour, "Robust co-optimization scheduling of electricity and natural gas systems via ADMM," *IEEE Trans. Sustain. Energy*. vol. 8, no. 2, pp. 658-670. Apr. 2017.
- [13] L. Bai, F. Li, T. Jiang, and H. Jia, "Robust scheduling for wind integrated energy systems considering gas pipeline and power transmission N-1 contingencies," *IEEE Trans. Power Syst.*, vol. 32, no. 2, pp. 1582-1584, Mar. 2017.
- [14] H. Cui, F. Li, Q. Hu, L. Bai, and X. Fang, "Day-ahead coordinated operation of utility-scale electricity and natural gas networks considering demand response based virtual power plants," *Appl. Energy*. vol. 176, pp. 183-195. Aug. 2016.
- [15] X. Zhang, M. Shahidehpour, A. Alabdulwahab, and A. Abusorrah, "Hourly electricity demand response in the stochastic day-ahead scheduling of coordinated electricity and natural gas networks," *IEEE Trans. Power Syst.*, vol. 31, no. 1, pp. 592-601, Jan. 2016.
- [16] L. Bai, F. Li, H. Cui, T. Jiang, H. Sun, and J. Zhu, "Interval optimization based operating strategy for gas-electricity integrated energy systems considering demand response and wind uncertainty," *Appl. Energy*. vol. 167, pp. 270-279. Apr. 2016.
- [17] C. Zhao and Y. Guan, "Data-driven stochastic unit commitment for integrating wind generation," *IEEE Trans. Power Syst.*, vol. 31, no. 4, pp. 2587-2596, Jul. 2016.
- [18] R. Jiang, Y. Guan, and J. Watson, "Risk-averse stochastic unit commitment with incomplete information," *IIE Trans.*, vol. 48, no. 9, pp. 838-854, 2016.
- [19] C. Duan, L. Jiang, W. Fang and J. Liu, "Data-Driven Affinely Adjustable Distributionally Robust Unit Commitment," *IEEE Trans. Power Syst.*, vol. 32, no. 2, pp. 1385-1398, Mar. 2018.
- [20] P. Xiong, P. Jirutitijaroen, and C. Singh, "A distributionally robust optimization model for unit commitment considering uncertain wind power generation," *IEEE Trans. Power Syst.*, vol. 32, no. 1, pp. 39-49, Jan. 2017.
- [21] B. Hu and L. Wu, "Robust SCUC considering continuous/discrete uncertainties and quick-start units: A two-stage robust optimization with mixed-integer recourse," *IEEE Trans. Power Syst.*, vol. 31, no. 2, pp. 1407-1419, Mar. 2016.
- [22] US DOT PHMSA, Guidance for pipeline flow reversals, product changes, and conversion to service, 2014, [Online]. Available: http://www.oc ceweb.com/PLS/2014Gas/Guide-Flo%20Rev-Prod%20Ch-Conver.pdf.
- [23] C. Zhao, J. Wang, J. P. Watson, and Y. Guan, "Multi-stage robust unit commitment considering wind and demand response uncertainties," *IEEE Trans. Power Syst.*, vol. 28, no. 3, pp. 2708-2717, Aug. 2013.
- [24] W. Wiesemann, D. Kuhn, and M. Sim, "Distributionally robust convex optimization," Oper. Res., vol. 62, no. 6, pp. 1358-1376, Oct. 2014.
- [25] C. Shang and F. You, "Distributionally robust optimization for planning and scheduling under uncertainty," *Comput. Chem. Eng.*, vol. 110, pp. 53-68. Feb. 2018.
- [26] D. Bertsimas, M. Sim, and M. Zhang, "Adaptive distributionally robust optimization," *Manag. Sci.*, (to appear).
- [27] A. Ben-Tal and A. Nemirovski, "Robust solutions of uncertain linear programs," Oper. Res. Lett., vol. 25, no. 1, pp. 1-13, Aug. 1999.
- [28] E. Read, B. Ring, S. Starkey, and W. Pepper, "An LP based market design for natural gas," in *Handbook of networks in power systems II*. Springer, 2012, pp. 77-113.

- [29] C. Wang, W. Wei, J. Wang and L. Wu, "Equilibrium of interdependent gas and electricity markets with marginal price based bilateral energy trading," *IEEE Trans. Power Syst.*, vol. 33, no. 5, pp. 4854-4867, Sept. 2018.
 [30] https://sites.google.com/view/chuanhe/testdata.